Light-Induced Decarbonylation, Solvolysis, and Isomerization of $Ru(L)(CO)_2Cl_2$ (L = 2,2′-Bipyridine and 4,4′-Dimethyl-2,2′-bipyridine) in Acetonitrile

Esa Eskelinen,[†] Matti Haukka,*[,†] Tapani Venäläinen,[†] Tapani A. Pakkanen,[†] Mikael Wasberg,[‡] Sylvie Chardon-Noblat,[§] and Alain Deronzier[§]

Department of Chemistry, University of Joensuu, P.O. Box 111, FIN-80101 Joensuu, Finland, Laboratory of Inorganic Chemistry, Åbo Akademi University, Biskopsgatan 8, FIN-20500 Åbo, Finland, and Laboratoire d'Electrochimie Organique et Photochimie Rédox, UMR 5630, Université Joseph Fourier, Grenoble 1, BP 53, 38041 Grenoble Cedex 9, France

Received July 19, 1999

The photochemical properties of Ru(II) mono(bipyridine) complexes $Ru(L)(CO)_2Cl_2$ [L = 2,2′-bipyridine (**1**, **2**) or 4,4′-dimethyl-2,2′-bipyridine (**3**)] were studied in CH_3CN and CH_2Cl_2. Photochemical ligand substitution reactions occurring in CH_3CN were followed by infrared and ^1H NMR spectroscopies and cyclic voltammetry. The structures of the photolysis products $Ru(bpy)(CO)(CH_3CN)Cl_2$ (**4**), *mer*-(CH_3CN) $Ru(bpy)(CH_3CN)_3Cl^+$ (**6**), and *fac*-(CH_3CN) $Ru(dmbpy)(CH_3CN)_3Cl^+$ (**8**) were determined by single-crystal X-ray crystallography. Photosubstitution of the *trans* (**1**) and *cis* (**2**) Cl isomers of $Ru(bpy)(CO)_2Cl_2$ (bpy = 2,2′-bipyridine) led to the same monosubstituted $Ru(bpy)(CO)(CH_3CN)Cl_2$ complex (**4**). Probably some isomerization occurs from the *trans* Cl isomer. Irradiation in CH_2Cl_2 led mainly to the dichloro-bridged $[Ru(bpy)(CO)Cl_2]_2$ (**5**) dimer starting from either the *trans* (**1**) or *cis* (**2**) isomer of $Ru(bpy)(CO)_2Cl_2$.

Introduction

Ruthenium polypyridine complexes are of great interest because of their redox properties and metal-to-ligand charge-transfer (MLCT) energies.[1,2] Ruthenium carbonyl mono(bipyridine) compounds[3] are attracting increasing attention despite the continuing popularity of the tris- and bis(bipyridine) complexes. The use of *trans*-(Cl) $Ru(bpy)(CO)_2Cl_2$ (bpy = 2,2′-bipyridine) as a starting material in halogen ligand exchange reactions has resulted in a variety of new complexes with differently substituted bipyridine ligands.[4−6] $Ru(bpy)(CO)_2Cl_2$ and its derivatives can also be modified by photo- and electrochemical means.[7−10]

Catalytic properties of $Ru(bpy)(CO)_2Cl_2$ and its derivatives have been tested in the photochemical[11] and electrochemical[12,13] reduction of CO_2, in the hydroformylation of 1-hexene and hydrogenation of 1-heptanal,[14] and most recently in the water-gas shift reaction.[15] Ruthenium bipyridine complexes undergo both ligand-based reductions and metal-based oxidations, which occur at high negative and positive potentials, respectively.[16] Addition of electron-donating or electron-accepting substituents to the bipyridine ligand is one way to control the potential of these redox reactions.[17] The reduction potential of a coordinated ligand has been found to correlate with metal-to-ligand charge-transfer energies. Thus, photo- and electrochemical studies where the electronic properties of the bipyridine ligands are varied promise to provide important insights into the mechanisms of catalytic processes, since the compounds formed may function as intermediates in catalytic cycles.[18,19]

* To whom correspondence should be addressed. E-mail: Matti.Haukka@joensuu.fi. Fax: +358-13-2513390.
[†] University of Joensuu.
[‡] Åbo Akademi University.
[§] Université Joseph Fourier.

(1) Juris, A.; Balzani, V.; Barigelletti, F.; Campagna, S.; Belser, P.; von Zelewsky, A. *Coord. Chem. Rev.* **1988**, *84*, 85.
(2) Kalyanasundaram, K., Grätzel, M., Eds. *Photosensitization and Photocatalysis Using Inorganic and Organometallic Compounds*; Kluwer Academic Publishers: Dordrecht, 1993.
(3) Haukka, M.; Kiviaho, J.; Ahlgrén, M.; Pakkanen, T. A. *Organometallics* **1995**, *14*, 825.
(4) Haukka, M.; Venäläinen, T.; Ahlgrén, M.; Pakkanen, T. A. *Inorg. Chem.* **1995**, *34*, 2931.
(5) Homanen, P.; Haukka, M.; Pakkanen, T. A.; Pursiainen, J.; Laitinen, R. H. *Organometallics* **1996**, *15*, 4081.
(6) Homanen, P.; Haukka, M.; Ahlgrén, M.; Pakkanen, T. A. *Inorg. Chem.* **1997**, *36*, 3794.
(7) Collomb-Dunand-Sauthier, M.-N.; Deronzier, A.; Ziessel, R. *J. Organomet. Chem.* **1993**, *444*, 191.
(8) Collomb-Dunand-Sauthier, M.-N.; Deronzier, A.; Ziessel, R. *J. Electroanal. Chem.* **1991**, *319*, 347.
(9) Collomb-Dunand-Sauthier, M.-N.; Deronzier, A.; Ziessel, R. *J. Electroanal. Chem.* **1993**, *350*, 43.
(10) Chardon-Noblat, S.; Deronzier, A.; Ziessel, R.; Zsoldos, D. *Inorg. Chem.* **1997**, *36*, 5384.
(11) Lehn, J.-M.; Ziessel, R. *J. Organomet. Chem.* **1990**, *382*, 157.
(12) (a) Collomb-Dunand-Sauthier, M.-N.; Deronzier, A.; Ziessel, R. *Inorg. Chem.* **1994**, *33*, 2961. (b) Ishida, H.; Fujiki, K.; Ohba, T.; Ohkubo, K.; Tanaka, K.; Terada, T.; Tanaka, T. *J. Chem. Soc., Dalton Trans.* **1990**, 2155.
(13) Collomb-Dunand-Sauthier, M.-N.; Deronzier, A.; Ziessel, R. *J. Chem. Soc., Chem. Commun.* **1994**, 189.
(14) Haukka, M.; Alvila, L.; Pakkanen, T. A. *J. Mol. Catal.* **1995**, *102*, 79.
(15) Haukka, M.; Venäläinen, T.; Kallinen, M.; Pakkanen, T. A. *J. Mol. Catal.* **1998**, *136* (2), 127.
(16) Balzani, V.; Juris, A.; Venturi, M.; Campagna, S.; Serroni, S. *Chem. Rev.* **1996**, *96*, 759.
(17) Caix-Cécillon, C.; Chardon-Noblat, S.; Deronzier, A.; Haukka, M.; Pakkanen, T. A.; Ziessel, R.; Zsoldos, D. *J. Electroanal. Chem.* **1999**, *466* (2), 187.
(18) Vlcek, A., Jr. *Chemtracts-Inorg. Chem.* **1993**, *5*, 1.
(19) Chardon-Noblat, S.; Deronzier, A.; Ziessel, R.; Zsoldos, D. *J. Electroanal. Chem.* **1998**, *444*, 253.

10.1021/om9905613 CCC: $19.00
Publication on Web 12/29/1999

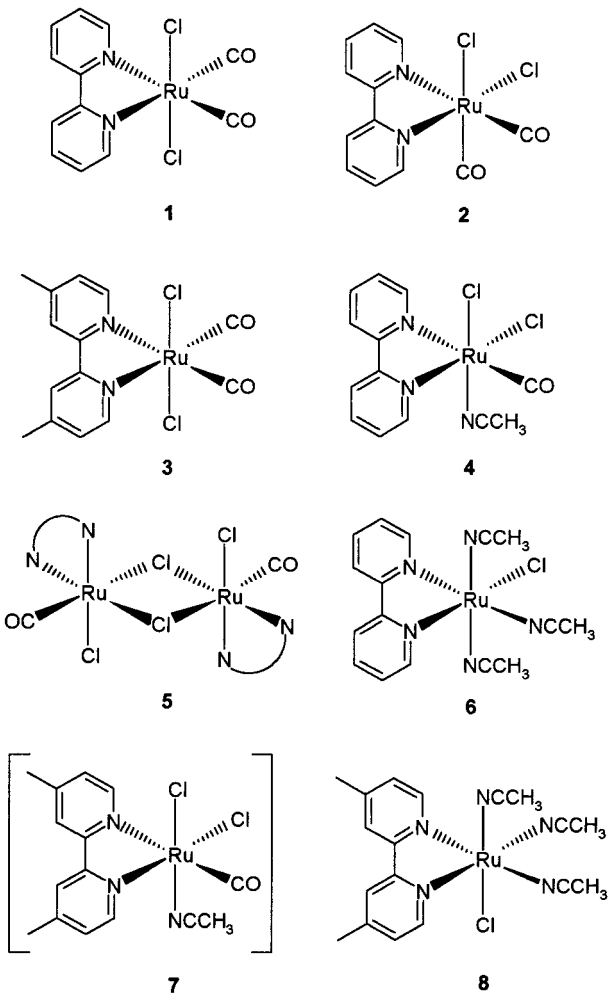

Figure 1. Structures of *trans*-(Cl) Ru(bpy)$(CO)_2Cl_2$ (**1**), *cis*-(Cl) Ru(bpy)$(CO)_2Cl_2$ (**2**), *trans*-(Cl) Ru(dmbpy)$(CO)_2Cl_2$ (**3**), *cis*-(Cl) Ru(bpy)$(CO)(CH_3CN)Cl_2$ (**4**), [Ru(bpy)$(CO)Cl_2]_2$ (**5**), *mer*-(CH_3CN) Ru(bpy)$(CH_3CN)_3Cl^+$ (**6**), *cis*-(Cl) Ru(dmbpy)-$(CO)(CH_3CN)Cl_2$ (**7**), and *fac*-(CH_3CN) Ru(dmbpy)$(CH_3$-$CN)_3Cl^+$ (**8**) (bpy = 2,2′-bipyridine; dmbpy = 4,4′-dimethyl-2,2′-bipyridine).

Photo- and electrochemical properties of Ru(bpy)-$(CO)_2Cl_2$ and some of its derivatives have been investigated earlier.[7−10] Previous studies[7] concerned with the photochemical reactivity of *trans*-(Cl) Ru(bpy)$(CO)_2Cl_2$ in acetonitrile have shown that, during photolysis, acetonitrile replaces both carbonyl ligands and one chloro ligand in three successive steps, giving rise to complexes Ru(bpy)$(CO)(CH_3CN)Cl_2$, Ru(bpy)$(CH_3CN)_2Cl_2$, and Ru(bpy)$(CH_3CN)_3Cl^+$.

In the present work, we investigated in detail the photochemical transformation of two ruthenium(II) mono(bipyridine) carbonyl complexes: Ru(bpy)$(CO)_2Cl_2$ (**1** and **2**) and Ru(dmbpy)$(CO)_2Cl_2$ (**3**; dmbpy = 4,4′-dimethyl-2,2′-bipyridine) (Figure 1). Photoirradiation has performed in coordinating (CH_3CN) and noncoordinating (CH_2Cl_2) solvent. The course of the reactions was followed by several spectroscopic methods together with cyclic voltammetry. We will show that photoirradiation of **1**−**3** results in ligand substitution in CH_3CN and in the formation of the dichloro-bridged dimer in CH_2Cl_2. Spiccia et al.[20] have recently reported that irradiation of *trans*-(Cl) Ru(L)$(CO)_2Cl_2$ (L = 2,2′-bipyridine analogue) in CH_2Cl_2 leads to the formation of a $[Ru(L)(CO)Cl_2]_2$ dimer. This will be discussed further in relation to our findings. Furthermore, we report here the photochemical reactivity of polymeric films $[Ru(L)-(CO)_2]_n$ (L = bpy, dmbpy).

Experimental Section

General Procedures. Acetonitrile (J.T. Baker, analytical grade) and tetrabutylammonium perchlorate (TBAP) (Fluka, electrochemical grade) were used as received. Cyclic voltammetry was performed under argon at room temperature in a three-electrode cell using an Autolab PGSTAT20 potentiostat-galvanostat. In all measurements a platinum disk (Metrohm, area 1.28 cm^2) was the working electrode and a platinum wire (Metrohm, length 0.5 cm) served as the counter electrode. Potentials are referred to a Ag/Ag^+ (0.01 mol/L) electrode in CH_3CN. Under the experimental conditions, the Fc^+/Fc (ferricinium ion/ferrocene) couple potential was 0.01 V. In all experiments, the potential scan rate was 100 mV s^{-1} and the $Ru(L)(CO)_2Cl_2$ concentrations were 2 mmol/L.

In photolysis experiments, all samples were irradiated under argon with a 450 W Xe-discharge lamp equipped with IR filter (Oriel model 8540). The desired wavelength (366 nm) was selected with a band-pass filter (Jobin-Yvon Type H 20 UV). The photolysis cell was a water-cooled vessel with a path length of 3 cm. Reactions were run in acetonitrile or dichloromethane, and progress of the reactions was monitored by the changes in IR and UV−vis spectra. For the cyclic voltammetry studies the resulting photolysis solutions were evaporated to dryness and the residue was dissolved in acetonitrile/TBAP solution.

Infrared spectra were measured with a Nicolet Magna 750 FTIR spectrometer. ^1H and ^{13}C NMR spectra were recorded at room temperature on a Bruker 250 MHz spectrometer using perdeuterated solvents as internal standard in CD_3CN (1.93 ppm), CD_2Cl_2 (5.24 ppm), and $CDCl_3$ (7.30 ppm). Elemental analyses were performed with an EA1110 CHNS-O (Carlo Erba Instruments) analyzer.

1. Spectroscopic Characterizations of Complexes 1−3. Ruthenium mono(bipyridine) compounds *trans*-(Cl) (**1**) and *cis*-(Cl) (**2**) Ru(bpy)$(CO)_2Cl_2$ isomers and *trans*-(Cl) Ru(dmbpy)-$(CO)_2Cl_2$ (**3**) were synthesized by literature methods.[3,10] ^1H NMR characterizations of complexes **1** and **2** are given in Figure 2 (A and C).

***trans*-(Cl) Ru(bpy)$(CO)_2Cl_2$ (1).** ^1H NMR in CD_3CN: δ = 9.17 (d, 2 $H_{66'}$), 8.47 (d, 2 $H_{33'}$), 8.24 (td, 2 $H_{44'}$), 7.74 (td, 2 $H_{55'}$); in CD_2Cl_2, δ = 9.16 (d, 2 $H_{66'}$), 8.29 (d, 2 $H_{33'}$), 8.17 (td, 2 $H_{44'}$), 7.70 (td,2 $H_{55'}$). FT-IR (cm^{-1}) in CH_3CN: 2064 (vs, ν_{CO}), 2001 (vs, ν_{CO}); in CH_2Cl_2, 2064 (vs, ν_{CO}), 2004 (vs, ν_{CO}). UV−vis (λ_{max} nm (ϵ, M^{-1} cm^{-1})) in CH_3CN: 352 (1614); in CH_2Cl_2, 362 (1583).

***cis*-(Cl) Ru(bpy)$(CO)_2Cl_2$ (2).** ^1H NMR in CD_3CN: δ = 9.52 (d, 1 H_6), 8.84 (d, 1 $H_{6'}$), 8.40 (2 d, 2 $H_{33'}$), 8.25 (td, 1 H_4), 8.13 (td, 1 $H_{4'}$), 7.79 (td, 1 H_5), 7.55 (td, 1 $H_{5'}$). FT-IR (cm^{-1}) in CH_3CN: 2067 (vs, ν_{CO}), 2001 (vs, ν_{CO}); in CH_2Cl_2, 2067 (vs, ν_{CO}), 2002 (vs, ν_{CO}). UV−vis (λ_{max} nm (ϵ, M^{-1} cm^{-1})) in CH_3CN: 352 (1319); in CH_2Cl_2, 362 (1363).

***trans*-(Cl) Ru(dmbpy)$(CO)_2Cl_2$ (3).** ^1H NMR in CD_3CN: δ = 8.96 (d, 2 $H_{66'}$), 8.30 (d, 2 $H_{33'}$), 7.54 (td, 2 $H_{55'}$), 2.57 (s, 6 H_{CH3}). FT-IR (cm^{-1} in CH_3CN): 2061 (vs, ν_{CO}), 1998 (vs, ν_{CO}). UV−vis (λ_{max} nm (ϵ, M^{-1} cm^{-1}) in CH_3CN): 340 (1715).

2. Characterizations of Complexes Formed in Photoirradiation of CH_3CN and CH_2Cl_2 Solutions of Initial Complexes. *cis*-(Cl) Ru(bpy)$(CO)(CH_3CN)Cl_2$ (4). ^1H NMR in CD_3CN: δ = 9.91 (d, 1 H_6), 9.09 (d, 1 $H_{6'}$), 8.44 (d, 1 H_3), 8.34 (d, 1 $H_{3'}$), 8.24 (t, 1 H_4), 7.95 (t, 1 $H_{4'}$), 7.84 (t, 1 H_5), 7.44 (t, 1 $H_{5'}$), 2.07 (s, 3 H_{CH3CN}). FT-IR (cm^{-1} in CH_3CN): 1969

(20) Deacon, G. B.; Kepert, C. M.; Sahely, N.; Skelton, B. W.; Spiccia, B.; Thomas, N. C.; White, A. H. *J. Chem. Soc., Dalton Trans.* **1999**, 275.

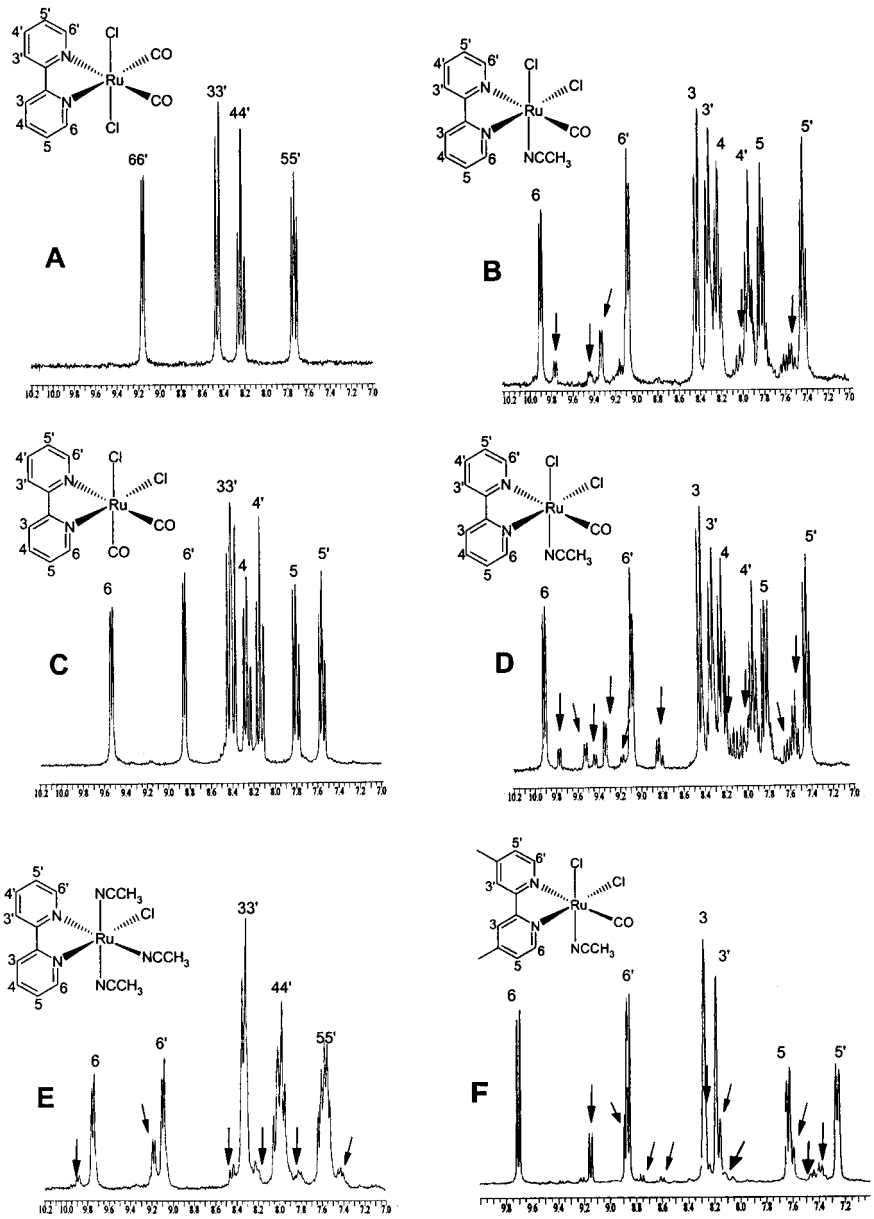

Figure 2. ^{1}H NMR characterizations of complexes (A) *trans*-(Cl) Ru(bpy)(CO)$_2$Cl$_2$ **(1)**, (B) *cis*-(Cl) Ru(bpy)(CO)(CH$_3$CN)-Cl$_2$ obtained by photolysis from **1**, (C) *cis*-(Cl) Ru(bpy)(CO)$_2$Cl$_2$ (**2**), (D) *cis*-(Cl) Ru(bpy)(CO)(CH$_3$CN)Cl$_2$ obtained by photolysis from **2**, (E) *mer*-(CH$_3$CN) Ru(bpy)(CH$_3$CN)$_3$Cl$^+$, and (F) *cis*-(Cl) Ru(dmbpy)(CO)(CH$_3$CN)Cl$_2$. The arrows indicate that some other complexes are formed in small quantities during photolysis.

(vs, ν_{CO}). UV−vis (λ_{max} in CH$_3$CN): 450 nm. Note: satisfactory elemental analysis was not obtained for this complex owing to impurities; see Figure 2B.

[Ru(bpy)(CO)Cl$_2$]$_2$ (5). FT-IR (cm^{-1} in CsI pellet): 1946 (s, ν_{CO}), 1931 (sh), 321 (w, ν_{RuCl}), 303 (w, ν_{Ru-Cl}). Note: ^{1}H NMR spectrum was not measured due to insolubility.

***mer*-(CH$_3$CN) Ru(bpy)(CH$_3$CN)$_3$Cl$^+$ (6).** ^{1}H NMR in CD$_3$CN: δ = 9.77 (d, 1 H$_6$), 9.12 (d, 1 H$_{6'}$), 8.36 (2 d, 2 H$_{33'}$), 8.03 (2 t, 2 H$_{44'}$), 7.60 (2 t, 2 H$_{55'}$), 2.12 (s, 3 H$_{CH3}$), 2.20 (s, 6 H$_{CH3}$). UV−vis (λ_{max} in CH$_3$CN): 438 nm. Anal. Calcd for [Ru-(bpy)(CH$_3$CN)$_3$Cl]$^+$Cl$^-$·3/2(CH$_2$Cl$_2$): C, 38.72; N, 12.91; H, 3.72. Found: C, 38.32; N, 13.31; H, 3.78.

Ru(dmbpy)(CO)(CH$_3$CN)Cl$_2$ (7). ^{1}H NMR in CD$_3$CN: δ = 9.71 (d, 1 H$_6$), 8.86 (d, 1 H), 8.28 (s, 1 H$_3$), 8.19 (s, 1 H$_{3'}$), 7.63 (d, 1 H$_5$), 7.25 (d, 1 H$_{5'}$), 2.60 (s, 3 H$_{CH3}$), 2.50 (s, 3 H$_{CH3}$), 2.06 (s, 3 H$_{CH3CN}$). FT-IR (cm^{-1} in CH$_3$CN): 1965 (vs, ν_{CO}). UV−vis (λ_{max} in CH$_3$CN): 444 nm. Anal. Calcd for Ru(dmbpy)(CO)-(CH$_3$CN)Cl$_2$·(CH$_3$CN)·(H$_2$O): C, 42.15; N, 11.57; H, 4.16. Found: C, 41.96; N, 11.49; H, 4.23. Note: The best fit was found with this composition; water was originated in nondried CH$_3$CN solvent .

***fac*-(CH$_3$CN) Ru(dmbpy)(CH$_3$CN)$_3$Cl$^+$ (8).** ^{1}H NMR in CDCl$_3$: δ = 9.69 (2 d, 2 H$_{66'}$), 8.20 (s, 2 H$_{33'}$), 7.35 (2 d, 2 H$_{55'}$), 2.68 (s, 6 H$_{CH3}$), 2.22 (s, 6 H$_{CH3CN}$), 2.18 (s, 3 H$_{CH3CN}$). Anal. Calcd for [Ru(dmbpy)(CH$_3$CN)$_3$Cl$^+$]Cl$^-$·7/4(H$_2$O): C, 42.31; N, 13.71; H, 4.84. Found: C, 42.61; N, 13.28; H, 4.62. Note: Again there were variable amounts of water in the bulk material even if only one water molecule was found in crystal structure.

3. Formation of Ru(bpy)(CO)(CH$_3$CN)Cl$_2$·CH$_2$Cl$_2$ (4), [Ru(bpy)(CH$_3$CN)$_3$Cl]$^+$Cl$^-$·3/2(CH$_2$Cl$_2$) (6), and [Ru-(dmbpy)(CH$_3$CN)$_3$Cl]$^+$Cl$^-$·(H$_2$O) (8) Crystals. A sample of Ru(bpy)(CO)$_2$Cl$_2$ (100 mg; 0.26 mmol) was dissolved in 30 mL of CH$_3$CN (8.7 mmol/L) and transferred to the photolysis reaction vessel. The solution was bubbled with Ar for approximately 15 min, and the photolysis was begun. After photolysis the reaction mixture was evaporated to dryness at room temperature, and the solid residue was dried in a vacuum. The residue was crystallized from CH$_2$Cl$_2$ for crystal-

Table 1. Crystallographic Data for Ru(bpy)(CO)(CH_3CN)Cl_2·CH_2Cl_2 (4), [Ru(bpy)(CH_3CN)$_3$Cl]$^+$$Cl^-$·3/2($CH_2Cl_2$) (6), and [Ru(dmbpy)($CH_3CN$)$_3$Cl]$^+$$Cl^-$·($H_2O$) (8)

	4	6	8
empirical formula	$C_{14}H_{13}Cl_4N_3ORu$	$C_{17.5}H_{20}Cl_5N_5Ru$	$C_{18}H_{23}Cl_2N_5ORu$
mol wt	482.14	578.71	497.38
cryst size, mm	0.1 × 0.1 × 0.2	0.05 × 0.1 × 0.2	0.2 × 0.2 × 0.1
cryst syst.	monoclinic	monoclinic	triclinic
space group	$P2_1/c$	$C2/c$	$P\bar{1}$
λ, Å	0.71073	0.71073	0.71073
a, Å	13.502(3)	31.650(2)	8.5255(8)
b, Å	12.615(3)	8.322(1)	10.1620(7)
c, Å	10.897(2)	18.228(1)	13.7879(13)
α, deg			70.710(6)
β, deg	93.13(3)	93.11(3)	72.801(5)
γ, deg			74.946(5)
V, Å^3	1853.3(7)	4794.0(7)	1059.51(16)
Z	4	8	2
D_{calc}, g/cm^3	1.728	1.604	1.559
μ mm^{-1}	1.427	1.225	1.009
T, K	293(2)	293(2)	150(2)
θ range, deg	2.95−25.00	2.78−24.99	2.54−25.30
no. of unique rflns	3242	4224	3815
no. of obsd data[a]	1935	2120	3260
no. of params	209	259	249
R1	0.0410	0.0422	0.0405
wR2	0.0880	0.0566	0.0877
largest diff peak and hole, e Å^{-3}	0.607 and −0.568	0.355 and −0.465	0.514 and −0.423

[a] $I > 2\sigma$.

lographic studies. The same procedure was used with the crystallization of **8**, only the starting complex was Ru(dmbpy)-$(CO)_2Cl_2$ (**3**).

4. X-ray Data Collection and Structure Solution for Ru(bpy)(CO)(CH_3CN)Cl_2·CH_2Cl_2 (4), [Ru(bpy)(CH_3CN)$_3$Cl]$^+$$Cl^-$·3/2($CH_2Cl_2$) (6), and [Ru(dmbpy)($CH_3CN$)$_3$Cl]$^+$$Cl^-$·($H_2O$) (8). All data were collected at 20 °C on a Nonius KappaCCD diffractometer using combined $\phi-\omega$-scan and Mo Kα radiation (λ = 0.71073 Å). Cell refinement and data reduction were done by Denzo and Scalepack programs.[21] The structures of **4** and **6** were solved by the Patterson heavy atom method with successive difference Fourier syntheses using the SHELXS-97 program.[22] The structure of **8** was solved by direct methods using the SIR97 program.[23] Structure refinement was carried out with the SHELXL-97 program.[24] All non-hydrogen atoms in **4**, **6**, and **8** were refined anisotropically. Organic hydrogens were placed in idealized positions and not refined (aromatic H: C−H = 0.93 Å at 293 K and 0.95 Å at 150 K, U_{iso} = 1.2U_{iso} of the parent carbon, CH_3 hydrogens in CH_3CN group: C−H = 0.96 Å at 293 K and 0.98 Å at 150 K, U_{iso} = 1.5U_{iso} of the parent carbon, CH_2 hydrogens in CH_2Cl_2: C−H = 0.97 Å, U_{iso}=1.2U_{iso} of the parent carbon). Hydrogens of water in **8** were located from the difference Fourier map but not refined. Crystallographic data are summarized in Table 1, and selected bond lengths and angles are given in Table 2.

Table 2. Selected Bond Lengths and Angles for Ru(bpy)(CO)(CH_3CN)Cl_2·CH_2Cl_2 (4), [Ru(bpy)(CH_3CN)$_3$Cl]$^+$$Cl^-$·3/2($CH_2Cl_2$) (6), and [Ru(dmbpy)($CH_3CN$)$_3$Cl]$^+$$Cl^-$·($H_2O$) (8)

	4	6	8
	Bonds (Å)		
Ru(1)−Cl(1)	2.3972(16)		
Ru(1)−Cl(2)	2.3989(18)	2.4345(15)	
Ru(1)−Cl(3)			2.3821(11)
Ru(1)−C(11)	1.925(6)		
Ru(1)−N(1)	2.114(4)	2.049(4)	2.032(3)
Ru(1)−N(2)	2.055(4)	2.038(4)	2.047(3)
Ru(1)−N(11)		2.028(4)	2.067(3)
Ru(1)−N(12)			2.055(4)
Ru(1)−N(13)		2.012(4)	
Ru(1)−N(15)	2.023(5)	2.012(4)	2.013(4)
C(11)−O(11)			
N(11)−C(11)		1.112(6)	1.103(5)
N(13)−C(13)		1.117(5)	
N(15)−C(15)	1.121(7)	1.129(5)	1.119(5)
N(12)−C(17)			1.109(5)
C(11)−C(12)		1.499(7)	1.492(6)
C(13)−C(14)		1.474(6)	
C(15)−C(16)	1.475(9)	1.461(6)	1.468(6)
C(17)−C(18)			1.484(6)
	Angles (deg)		
N(1)−Ru(1)−N(2)	77.82(16)	79.42(17)	79.23(12)
Ru(1)−C(11)−O(11)	177.6(7)		
N(11)−C(11)−C(12)		178.9(7)	178.4(5)
N(13)−C(13)−C(14)		179.0(7)	
N(15)−C(15)−C(16)	179.0(7)	179.2(6)	178.2(4)
N(12)−C(17)−C(18)			178.6(5)

Results and Discussion

A. Formation of Ru(L)(CO)(CH_3CN)Cl_2 [L = bpy (4) or dmbpy (7)] from *trans*-(Cl) Ru(L)$(CO)_2Cl_2$ [L = bpy (1) or dmbpy (3)] and *cis*-(Cl) Ru(L)$(CO)_2Cl_2$ (2) in CH_3CN. Before photolysis, the IR spectrum showed ν(CO) stretching bands at 2064 and 2001 cm^{-1} for complex **1** (Figure 3) and at 2061 and 1998 cm^{-1} for complex **3**. Immediately after start of the photolysis the solutions turned from light yellow to red and at the same time a new peak appeared: ν(CO) = 1969 cm^{-1} for **1** and 1965 cm^{-1} for **3**. Photolysis reactions were carried out until the two original peaks had disappeared and only the new peak remained in the carbonyl stretching region.

As previously reported,[9,17] the cyclic voltammograms of the initial solutions of *trans*-(Cl) complexes **1** and **3** exhibit an almost fully reversible system [for **1** $E_{1/2}$ =

(21) Otwinowski, Z.; Minor, W. In *Methods in Enzymology, Vol. 276, Macromolecular Crystallography, Part A*; Carter, C. W., Jr., Sweet, R. M., Eds.; Academic Press: New York, 1997; pp 307−326.
(22) Sheldrick, G. M. *SHELXS97*, Program for Crystal Structure Determination; University of Göttingen, 1997.
(23) Altomare, A.; Cascarano, C.; Giacovazzo, C.; Guagliardi, A.; Moliterni, A. G. G.; Burna M. C.; Polidori, G.; Camalli, M.; Spagna, R. *SIR97*, A Package for Crystal Structure Solution by Direct Methods and Refinement; University of Bari, Italy, 1997.
(24) Sheldrick, G. M. *SHELXL97*, Program for Crystal Structure Refinement; University of Göttingen, 1997.

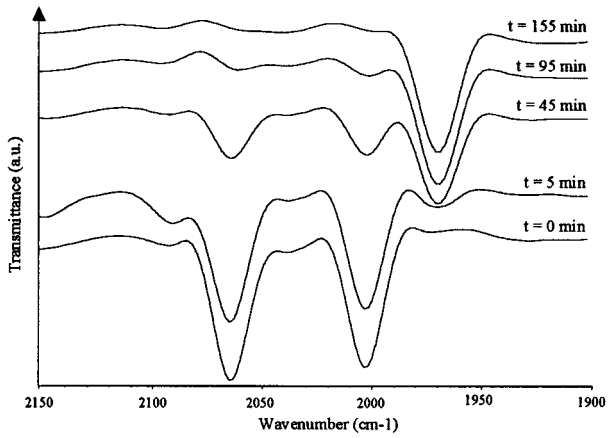

Figure 3. Changes in the IR spectra of *trans*-(Cl) Ru(bpy)(CO)$_2$Cl$_2$ **(1)** during photolysis and formation of Ru(bpy)(CO)(CH$_3$CN)Cl$_2$ **(4)**.

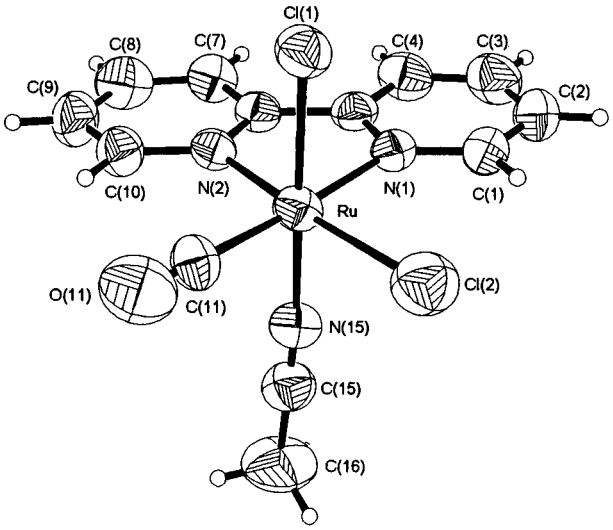

Figure 4. Structure of Ru(bpy)(CO)(CH$_3$CN)Cl$_2$ **(4)**.

1.47 V, ΔE_p = 112 mV; for **3** $E_{1/2}$ = 1.41 V, ΔE_p = 127 mV] corresponding to the Ru(II)/Ru(III) conversion of the oxidation state of the metal. After photolysis, the voltammograms of **4** and **7** showed a new reversible Ru(II)/Ru(III) system [$E_{1/2}$ = 0.78 V, ΔE_p = 92 mV for **4**; $E_{1/2}$ = 0.74 V, ΔE_p = 138 mV for **7**], while the initial peak system had disappeared. The redox potentials of these new peak systems were approximately the same as those obtained[9] for Ru(bpy)(CO)(CH$_3$CN)$_2$Cl^{2+} after oxidation of Ru(bpy)(CO)$_2$Cl$_2$ solution at positive potentials without photolysis. Furthermore, without additional photoirradiation the same kinds of changes in the IR spectra and cyclic voltammograms were observed for the solutions after a 2-month exposure to normal laboratory light.

The crystal structure of orange-brown **4** confirmed the result obtained for the photolysis reaction and revealed that the single acetonitrile ligand was positioned *trans* to the chloro ligand (Figure 4). Crystallization of Ru(dmbpy)(CO)(CH$_3$CN)Cl$_2$ **(7)** did not succeed, but the similarity of the IR and NMR spectra and cyclic voltammograms of **4** and **7** suggest that the structure of **7** is similar to that of **4**. The ^{1}H NMR spectra of a solution of the *trans*-(Cl) Ru(bpy)(CO)$_2$Cl$_2$ before and after photoirradiation are shown in Figure 2A,B. The spectra are noticeably different. This difference is similar to that observed between the ^{1}H NMR spectra of *trans* and *cis* isomers of the initial chloro complexes [**1** and **2**; Figure 2A,C]. The symmetry of the complexes defines the number of sets for aromatic bipyridine protons.

The ^{1}H NMR spectrum of *trans*-(Cl) Ru(bpy)(CO)$_2$Cl$_2$ in CD$_3$CN (Figure 2A) showed only four resonances, consistent with the symmetrical pattern for the bipyridine chelator. After irradiation, eight new sets for aromatic protons (Figure 2B) were observed. This peak splitting in the second spectrum indicates the presence of different ligands in *trans* positions relative to the bpy nitrogens. Thus, the spectra collected before and after photosubstitution are in good agreement with the structure of **4** shown in Figure 4. The NMR spectrum confirms that an isomerization occurs during the decarbonylation−acetonitrile coordination photoprocess. Since a geometrical change occurred during the photosubstitution of the *trans*-(Cl) isomer, it was relevant to study the irradiation of the *cis*-(Cl) isomer **(2)** under the same conditions. Photolysis of the *cis*-(Cl) Ru(bpy)(CO)$_2$Cl$_2$ **(2)** complex led to the release of one carbonyl ligand and the recoordination of a solvent molecule without rearrangement of the initial *cis* chloro geometry. Effectively the IR, UV−vis, and ^{1}H NMR spectroscopies establish that the complex **4** obtained by photoirradiation of the *cis* chloro isomer is identical in structure to that obtained from the *trans* chloro isomer (for the ^{1}H NMR experiment see Figure 2D).

B. Photoirradiation of *cis* and *trans* Isomers of Ru(bpy)(CO)$_2$Cl$_2$ in CH$_2$Cl$_2$. To complete this study, we also investigated the photoirradiation of the two Ru(bpy)(CO)$_2$Cl$_2$ isomers in a noncoordinating solvent, CH$_2$Cl$_2$. Here the two isomers have a similar photoreactivity, which leads to the formation of new low-solubility complexes resulting from a monodecarbonylation. It has recently been demonstrated by X-ray structure characterization that the photodecarbonylation of the Ru(L)(CO)$_2$Cl$_2$ [L = di(2-pyridyl)ketone(dpk) and 1,10-phenantroline(phen)] *trans* chloro isomers leads mainly to the formation of chloro-bridged dimers with structures like **5** (Figure 1).[20]

The photoirradiation of **1** in CH$_2$Cl$_2$ led to the dimer **5**, which shows a single carbonyl band at 1946 cm^{-1} with shoulder at 1931 cm^{-1}. The same behavior has been observed earlier in irradiation of complexes Ru(L)(CO)$_2$Cl$_2$ (L = bpy, dmbpy, and phen). Photo-monodecarbonylation resulted in low-solubility dimers with structures such as **5** with CO bands located at ca. 1945 cm^{-1}.[20] A more complex monodecarbonylation takes place for the *cis* chloro isomer **(2)**. The IR and UV−vis spectra recorded at regular intervals during the photolysis of **2** showed regular weakening of the ν(CO) signals at 2067 and 2002 cm^{-1} (cf. CsI pellets 2067 and 1998 cm^{-1}) and of the maximum absorption at 362 nm, respectively. Consumption of the initial complex was coupled with the appearance of a suspension of an orange precipitate, which was fully insoluble in most common organic solvents. The FT-IR spectrum showed carbonyl bands of similar intensity at 1954 and 1946 cm^{-1} with shoulders at 1967 and 1931 cm^{-1}, respectively. Evidently, irradiation of the *cis* chloro isomer produces the dimer **5**, along with another dimer of different structure. The insolubility of the precipitate

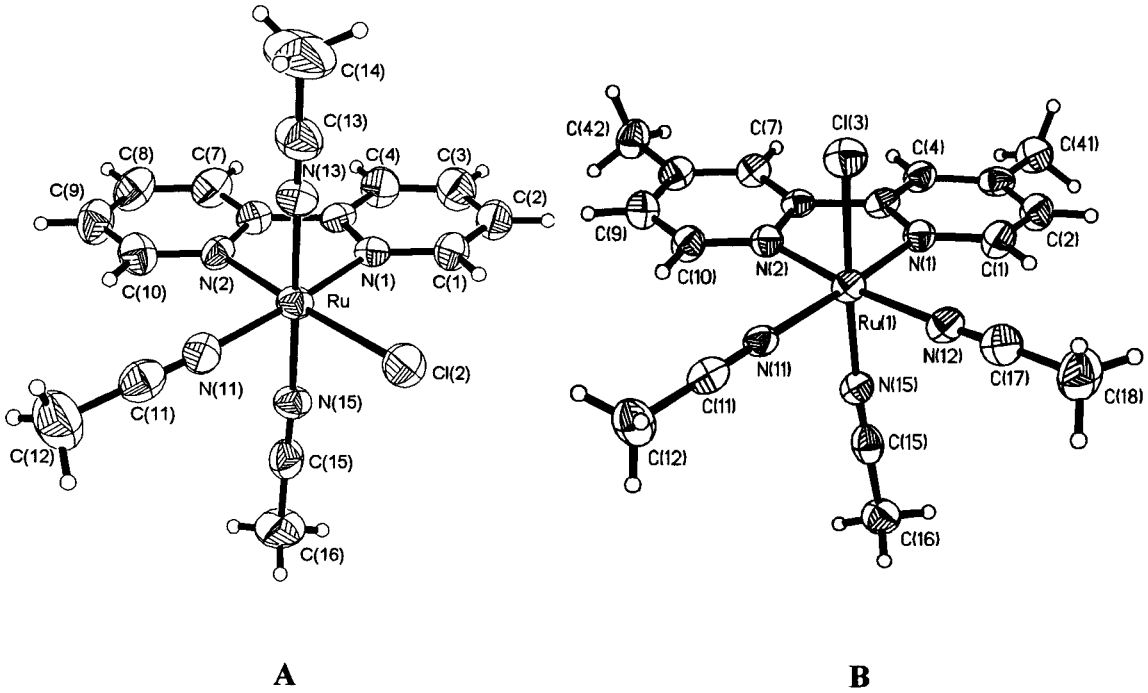

Figure 5. Structures of (A) Ru(bpy)$(CH_3CN)_3Cl^+$ (**6**) and (B) Ru(dmbpy)$(CH_3CN)_3Cl^+$ (**8**).

prevented the separation of these two compounds and structure analysis by X-ray diffraction.

C. Formation of Ru(L)$(CH_3CN)_3Cl^+$ [L = bpy (6) or dmbpy (8)]. Photolysis of *trans*-(Cl) Ru(L)$(CO)_2Cl_2$ was continued after step **A** until the carbonyl peaks at 1969 cm^{-1} [Ru(bpy)$(CO)_2Cl_2$ (**1**)] and 1965 cm^{-1} [Ru(dmbpy)$(CO)_2Cl_2$ (**2**)] had disappeared. At the end of the photolysis both solutions were deep red. Cyclic voltammograms of the two solutions exhibited reversible wave systems at 0.74 and 0.71 V for **6** and **8**, respectively, corresponding to the metal oxidation Ru(II)/Ru(III) in Ru(L)$(CH_3CN)_3Cl^+$ complexes, as previously reported for **1**.[7] Single-crystal X-ray analysis of the crystals revealed the crystal structures shown in Figure 5. This provided additional evidence for the final products in photolysis reaction: two of the linear acetonitrile ligands are located in different positions. The structures were confirmed by elemental analyses and ^1H NMR spectroscopy (Figure 2E). The spectrum presents an unsymmetrical complex arrangement of eight resonances for the aromatic protons.

The mechanisms of the above-mentioned photochemical ligand exchange reactions are not accurately known, and we suggest the reaction sequences shown in Scheme 1. The reaction involves in both solvents as a first step photodissociation of one equatorial CO ligand. In noncoordinating CH_2Cl_2 solvent (Scheme 1B) reaction proceeds through a five-coordinate intermediate, which is supported by the fact that dinuclear complex **5** is formed. The photolysis of Ru(L)$(CO)_2Cl_2$ in the coordinating solvent CH_3CN did not produce any dinuclear complexes; only the monosubstituted CH_3CN complexes were observed. The dimerization of the unsaturated complex does not occur in CH_3CN probably because the coordination of CH_3CN is faster than the dimerization, since CH_3CN is in large excess. However, since no dimer **5** was formed, there is no unambiguous evidence of the rearrangement mechanism (Scheme 1A). The isomerism of the starting complex [*trans*-(Cl) **(1)** or *cis*-(Cl) **(2)**] has no effect on the structure of the final mono(CH_3CN)-substituted complex **(4)**. The most likely mechanism for the formation of **4** is the primary photodissociation of an axial CO ligand followed by a coordination reaction.

The structures of the triple acetonitrile-substituted $[Ru(L)(CH_3CN)_3Cl]^+$ complexes **6** and **8** indicate that photolysis results in additional isomerization. The only Cl ligand can be located in different positions, which means that the isomeric form of the starting compound is not straightforward. Furthermore, it should be recalled[7] that the formation of one possible intermediate, $Ru(CH_3CN)_2Cl_2$, is not quantitative. The mixture of photodecarbonylated complexes may also give rise to the different isomeric forms of the end products.

Photochemical Behavior of $[Ru(L)(CO)_2]_n$ (L = bpy or dmbpy). The electrochemistry of Ru(L)$(CO)_2Cl_2$ at negative potentials is mainly governed by the formation and reactions of polymeric $[Ru(L)(CO)_2]_n$ films.[12a,13,17,25] In a typical cyclic voltammogram of **3**, the irreversible cathodic peak ($E_{pc} = -1.62$ V) corresponds to the formation and the anodic peak ($E_{pa} = -0.85$ V) to the dissolution of the polymeric, black, air-sensitive $[Ru(dmbpy)(CO)_2]_n$ material on the working electrode according to reaction 1.[17]

$$n\ Ru^{II}(dmbpy)(CO)_2Cl_2 + 2n\ e^- \rightarrow [Ru^0(dmbpy)(CO)_2]_n + 2n\ Cl^- \quad (1)$$

We discovered that the organometallic polymer films $[Ru(L)(CO)_2]_n$ (L = bpy or dmbpy) are reactive toward light. If, for example, the $[Ru(bpy)(CO)_2]_n$ film deposited on a working electrode in the original Ru(bpy)$(CO)_2Cl_2$ solution is photolyzed, the measured current will increase markedly from the constant value. When the light is switched off, the current will return to its

(25) Chardon-Noblat, S.; Deronzier, A.; Zsoldos, D.; Ziessel, R.; Haukka, M.; Pakkanen, T.; Venäläinen, T. *J. Chem. Soc., Dalton Trans.* **1996**, 2581.

Scheme 1

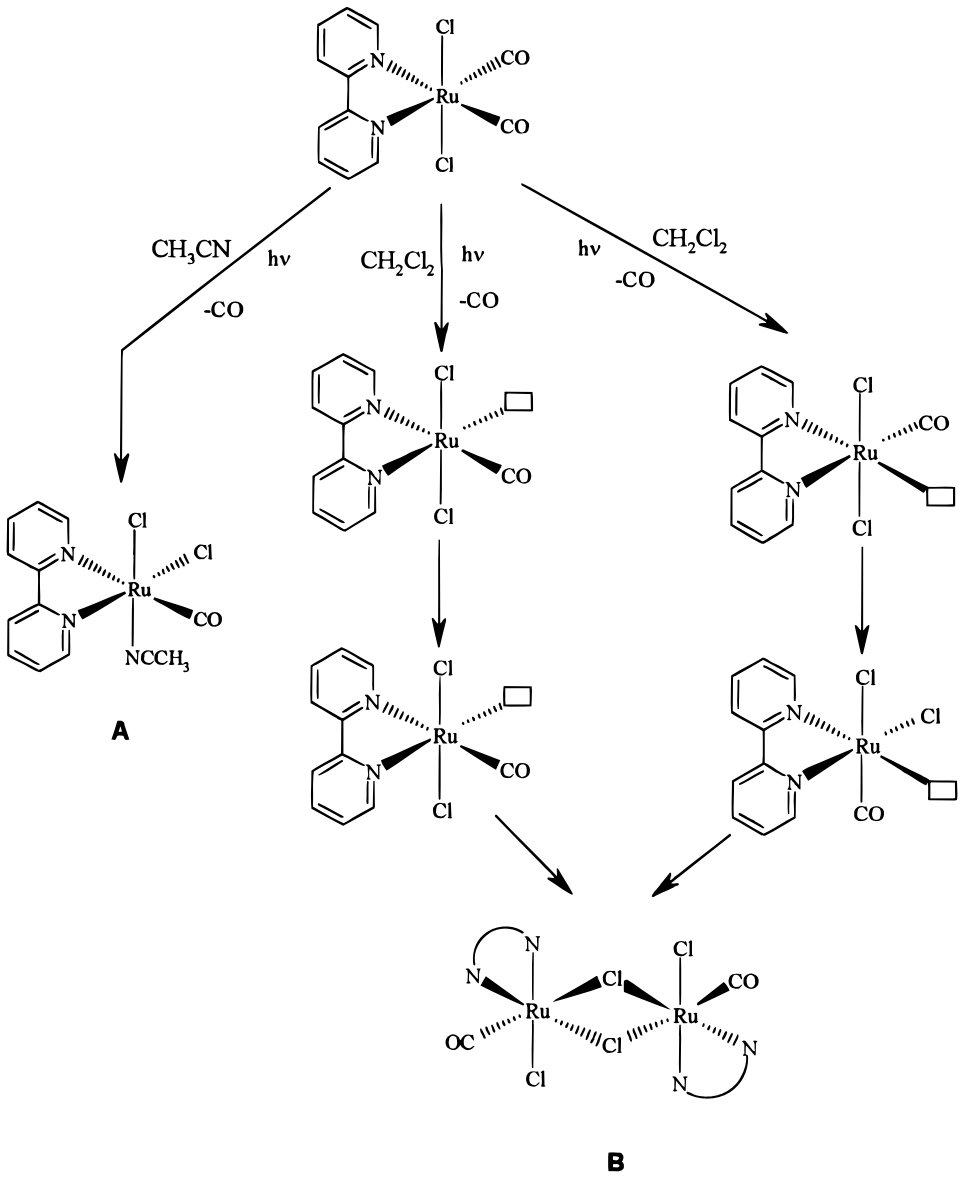

original value. Requirements for this phenomenon are as follows: (1) The potential range of the working electrode must be adjusted to the value at which the polymer film grows ($E_{pc} < -1.6$ V for Ru(L)(CO)$_2$Cl$_2$). It is essential that there is a polymer film on the working electrode; with the bare working electrode in the same solution no changes in the current occur. (2) The external light must be exactly focused on the polymer film. Further attempts will be made to clarify this phenomenon.

Conclusion

Physicochemical characterizations of the structures of complexes formed by ligand substitution under photoirradiation in CH_3CN showed that rearrangements of the ligands occur simultaneously. The complexes Ru(L)(CO)$_2$Cl$_2$ undergo immediate photosubstitution with the coordinating solvent (CH_3CN). The same mono-(CH_3CN)-substituted complex Ru(L)(CO)(CH_3CN)Cl$_2$ was obtained starting from the *trans*- and *cis*-(Cl) isomers. In the formation of the *cis*-(Cl) Ru(bpy)(CO)(CH_3CN)Cl$_2$ complex **(4)**, for instance, one axial chloro ligand of the initial complex **(1)** moved to an equatorial position. In noncoordinating solvent (CH_2Cl_2), irradiation led mainly to dichloro-bridged [Ru(L)(CO)Cl$_2$]$_2$ complexes, resulting from isomerization coupled with ejection of carbonyl ligands. The polymer films [Ru(L)(CO)$_2$]$_n$ (L = bpy or dmbpy) deposited on a working electrode at negative potentials showed photochemical reactivity. This reactivity could be observed as reversible current changes under exposure to light, and it is an intrinsic property of these polymeric ruthenium films.

Supporting Information Available: Further details of the crystal structure determination including tables of crystal data and structure refinement, atomic coordinates, bond lengths and angles, and thermal parameters, and figures showing the cyclic voltammograms of Ru(L)(CO)(CH_3CN)Cl$_2$ (L = bpy, dmbpy) at positive and Ru(dmbpy)(CO)$_2$Cl$_2$ at negative potentials, and the ^{1}H NMR spectrum of Ru(dmbpy)(CH_3CN)$_3$Cl$^+$. This material is available free of charge via the Internet at http://pubs.acs.org.

OM9905613